Mössbauer-Zeeman ^{57}Fe spectroscopy using nuclear ground states dressed with RF photons

1998 J. Phys.: Condens. Matter 10 9507

(http://iopscience.iop.org/0953-8984/10/42/016)

J. Phys.: Condens. Matter **10** (1998) 9507–9524. Printed in the UK PII: S0953-8984(98)93532-9

Mössbauer–Zeeman ^{57}Fe spectroscopy using nuclear ground states dressed with RF photons

Jos Odeurs† and Gilbert R Hoy‡

† Katholieke Universiteit Leuven, Instituut voor Kern-en Stralingsfysica, Celestijnenlaan 200 D, B-3001 Leuven, Belgium

‡ Physics Department, Old Dominion University, Norfolk, VA 23529-0458, USA

Received 22 April 1998, in final form 2 July 1998

Abstract. As part of our general programme to develop the field of quantum nucleonics, we have studied Mössbauer spectroscopy when there is Zeeman splitting of the nuclear levels and a further interaction due to an applied rf-radiation field. We have applied the 'dressed' state concept, developed in quantum electronics, to this situation. In particular, we have studied the case when the rf frequency is in the neighbourhood of the ground state (spin $= 1/2$) splitting. The dressed-state approach in this case treats the coupling of nuclear Zeeman levels, due to an rf field, by considering the total system made up of nucleus, static magnetic field and rf field as one global quantum system. This allows the time evolution of the system to be handled straightforwardly. The energy levels and corresponding eigenstates of the system are calculated as a function of the rf frequency and the magnitude of the rf magnetic flux density. Mössbauer spectra are calculated for the ^{57}Fe case in which the source is subjected to both the static and radiation fields while the absorber nuclear levels are unsplit. Spectra are given as a function of the rf frequency, the magnitude of rf-field magnetic flux density, as well as the photon direction.

1. Introduction

The concept of a 'dressed' atomic state has been developed in the field of quantum electronics [1–3]. [3] gives a very complete description of the dressed-state concept in the quantum-electronics context. The interaction between the atomic system and the radiation electromagnetic field is treated in a fashion in which both the atomic system and the radiation electromagnetic field are quantum systems. Next the two quantum systems are combined into one global quantum system. For this global quantum system the Hamiltonian is time independent. Thus the time evolution of the global system is easily described in terms of the usual time evolution operator. We are interested in applying these techniques, so successfully developed in quantum electronics, to cases involving nuclei. This field has recently been termed 'quantum nucleonics'. In a previous series of publications [4–7] the concept of a 'dressed' nucleus has been introduced in order to describe the interaction of a nucleus with a radiation field where the 'dressing' is in the excited nuclear state. An analogous study can be performed when the radiation field couples the two Zeeman split sub-levels of the nuclear ground state having spin $(I_g) = 1/2$. This is the subject of this paper. We will show how the ^{57}Fe-Mössbauer spectrum, using a single-line absorber and a source 'dressed' in the ground state with rf photons, changes as a function of frequency and strength of the rf field. We consider the case when the direction of the static Zeeman magnetic field and photon emission direction lie in a plane perpendicular to the magnetic flux

0953-8984/98/429507+18$19.50

density of the rf radiation. In this article a case more general than previously considered will be treated, in which the static Zeeman magnetic field is not necessarily along the direction of the emitted photons. Of particular interest is the situation when the frequency of the rf signal approaches the resonance condition, i.e. matches the frequency of the ground-state Zeeman splitting.

The main motivation for the study of the interaction of radio-frequency fields and nuclei using the completely quantum-mechanical description is, as mentioned above, due to the emerging discipline of quantum nucleonics. The development of a gamma-ray laser would be the pinnacle of this research [8]. The completely quantum-mechanical study has the advantage that all operators are time independent (Schrödinger picture). This is possible because the system consisting of nucleus + static magnetic field + rf field can be considered as one global quantum system. Conceptually, as well as numerically, this approach differs from the other studies (see references in section 5 below), where the radio-frequency field is taken as a classical one. The results from both approaches are equivalent, although the results based on the quantum-mechanical study can be obtained in a simpler and more elegant way and, as a consequence, should prove useful in the further development of quantum nucleonics.

The paper is divided into six sections. Section 2 treats the familiar case when the ^{57}Fe nuclei are in a static magnetic field in the absence of any rf field. The nuclear energy levels and eigenstates, for the first-excited and ground states, are indicated in this simple case. This section provides an opportunity to introduce the notation used in subsequent sections. In section 3 the new nuclear energy levels and eigenstates are determined when the additional rf radiation is applied producing the so-called 'dressed states' in the nuclear ground states. A brief discussion of the time evolution of the nuclear ground states and the connection to Rabi oscillations is also presented. In section 4 the spontaneous emission of the ^{57}Fe source from the first-excited state levels to the 'dressed' ground state levels is calculated. Then, assuming an unsplit, i.e. single-line, ^{57}Fe absorber, representative Mössbauer transmission spectra are simulated. Section 5 contains some additional discussions and section 6 gives conclusions.

2. Nuclear energy eigenvalues and eigenstates in the absence of rf coupling

Let us consider a nucleus in a static magnetic field in the absence of the rf-radiation field. The interaction Hamiltonian is simply the usual magnetic dipole interaction. The excited state is labelled by e and the ground state is labelled g. The excited- and ground-state magnetic dipole moments are $\boldsymbol{\mu}_e$ and $\boldsymbol{\mu}_g$, and $\boldsymbol{B}_0$ is the static Zeeman magnetic field taken to be along the z'-axis. (Another z-axis is introduced later, thus the z' here.)

The Hamiltonian is diagonal in the z'-axis system, and the eigenstates are 'pure' m-states. The nuclear spin of the first excited state of ^{57}Fe (I_e) is 3/2 and that of the ground state (I_g) is 1/2. The energies of the nuclear states in the absence of the rf radiation are simply

$$\begin{aligned} E_{e,m'_e} &= E_0 + |\gamma_e| B_0 m'_e \\ E_{g,m'_g} &= -\gamma_g B_0 m'_g \end{aligned} \tag{1}$$

where the magnetic moments of the excited and ground states are given by

$$\boldsymbol{\mu}_e = \gamma_e \boldsymbol{I}_e \text{ and } \boldsymbol{\mu}_g = \gamma_g \boldsymbol{I}_g \tag{2}$$

and γ_e, the excited-state gyromagnetic ratio, is negative while γ_g, the ground-state gyromagnetic ratio, is positive for ^{57}Fe.

The corresponding eigenstates in the z'-axis system can be written simply as

$$|3/2, m'_e\rangle \text{ and } |1/2, m'_g\rangle. \tag{3}$$

These eigenstates are nothing more than the familiar nuclear Zeeman states. In the next section we introduce the applied rf field.

3. Energy eigenvalues and eigenstates of the 'dressed' nucleus

3.1. General expressions

Now let us consider the nucleus in a static magnetic field and add the presence of n photons corresponding to one mode of the radiation field. For the moment we will not consider the excited nuclear states. This is because the radiation field only has a significant role when the rf frequency is close to the resonance condition. In the absence of any interaction between the nucleus and the radiation field, the total Hamiltonian for the ground state can be written

$$H_g = -\boldsymbol{\mu}_g \cdot \boldsymbol{B}_0 + \hbar\omega(a^+a + \tfrac{1}{2}) \tag{4}$$

where the only additional features are ω, the frequency of the rf field, and a^+ and a, the usual creation and annihilation operators of the rf-radiation field. Neglecting at this stage any interaction between the nuclear ground states and the rf-radiation field, the eigenstates of this system are the direct product of the nuclear eigenstates, given above, and the rf-radiation eigenstates. The eigenstates of the rf-radiation field are commonly written $|n\rangle$, where n is the eigenvalue of the number operator a^+a.

There are two situations that we must consider. First we consider (case 1) the situation in which the nucleus is in the lowest ground-state nuclear energy level, namely $|1/2, 1/2'\rangle$, and there are n photons in the radiation field. The complete state is denoted $|1/2, 1/2'\rangle \otimes |n\rangle$. There is another state of approximately the same energy. This state is the one in which the nucleus is in its higher ground-state level and there is one less photon in the rf field. This state is represented by $|1/2, -1/2'\rangle \otimes |n-1\rangle$. Thus, for this condition, we introduce two orthonormal states defined as

$$|\varphi_1\rangle = |1/2, 1/2'\rangle \otimes |n\rangle \text{ and } |\varphi_2\rangle = |1/2, -1/2'\rangle \otimes |n-1\rangle. \tag{5}$$

Unless the sample is at a very low temperature, such that only the lowest nuclear ground state is occupied, we have the additional possibility (case 2) that the system is in the upper ground-state nuclear level when there are n photons in the rf-radiation field. In this case the nucleus can emit an rf photon, return to the lower nuclear ground state and increase the number of photons in the field by one. So, for this condition, we introduce an additional set of two orthonormal states defined as

$$|\varphi'_1\rangle = |1/2, -1/2'\rangle \otimes |n\rangle \text{ and } |\varphi'_2\rangle = |1/2, 1/2'\rangle \otimes |n+1\rangle. \tag{6}$$

3.1.1. Case 1. For the two-dimensional vector space spanned by this set, namely (5), one can write down immediately the energy eigenvalues in the absence of rf coupling

$$\begin{aligned} &|\varphi_1\rangle \text{ has energy } E_{1g} = -\tfrac{1}{2}\gamma_g\hbar B_0 + \hbar\omega(n + \tfrac{1}{2}) \\ &|\varphi_2\rangle \text{ has energy } E_{2g} = \tfrac{1}{2}\gamma_g\hbar B_0 + \hbar\omega(n - \tfrac{1}{2}). \end{aligned} \tag{7}$$

The energy difference is then:

$$E_{2g} - E_{1g} = \gamma_g\hbar B_0 - \hbar\omega \tag{8}$$

and we will set $\gamma_g B_0 = \omega_g$ so

$$E_{2g} - E_{1g} = \hbar\Delta\omega \text{ where } \Delta\omega = \omega_g - \omega. \tag{9}$$

Since γ_g is positive, $\omega_g > 0$.

At resonance $\Delta\omega = 0$ and $E_{1g} = E_{2g}$. This energy has then a twofold degeneracy.

Now we introduce the interaction between the rf-radiation field and the two nuclear ground-state Zeeman sublevels, i.e. the two orthonormal vectors in our space. This interaction is described by the interaction Hamiltonian H_{int} given by

$$H_{\text{int}} - \boldsymbol{\mu}_g \cdot \boldsymbol{B}_{rf} \tag{10}$$

where the magnetic flux density $\boldsymbol{B}_{rf}$ of the rf-radiation field is given by [9]

$$\boldsymbol{B}_{rf} = -\frac{\mathrm{i}}{c}\sqrt{\frac{\hbar\omega}{2\varepsilon_0 V}}(\varepsilon a\, \mathrm{e}^{\mathrm{i}\boldsymbol{k}\cdot\boldsymbol{r}} - \varepsilon^* a^+ \mathrm{e}^{-\mathrm{i}\boldsymbol{k}\cdot\boldsymbol{r}}) \times \boldsymbol{u}_{\boldsymbol{k}}. \tag{11}$$

In (11) V is the (cubic) volume in which the rf-radiation field is generated, ε is the unit vector (real or complex) describing the polarization of the photons, $\boldsymbol{k}$ is the photon wavevector with $|\boldsymbol{k}| = \omega/c$ and $\boldsymbol{u}_{\boldsymbol{k}} = \boldsymbol{k}/|k|$. In the usual long wavelength limit ($\mathrm{e}^{\pm\boldsymbol{k}\cdot\boldsymbol{r}} \approx 1$), and using (2), (10) becomes

$$H_{\text{int}} = \frac{\mathrm{i}}{c}\gamma_g\hbar\sqrt{\frac{\hbar\omega}{2\varepsilon_0 V}}\boldsymbol{I}_g \cdot (\varepsilon a - \varepsilon^* a^+) \times \boldsymbol{u}_{\boldsymbol{k}}. \tag{12}$$

All operators are time-independent (Schrödinger picture). In order to proceed we have to specify the polarization of the rf-radiation field and hence the direction of the rf magnetic flux density. We will chose the polarization to be linear and the rf magnetic flux density to be along the y'-axis, i.e.

$$\varepsilon \times \boldsymbol{u}_{\boldsymbol{k}} = \boldsymbol{u}'_y \tag{13}$$

where $\boldsymbol{u}'_y$ is a unit vector in the direction of the y'-axis, which is perpendicular to the static magnetic field $\boldsymbol{B}_0$, which is along the z'-axis. A still more general case could be treated. This, however, would make the resulting expressions more cumbersome although the analysis is straightforward. With the specified polarization of the rf-radiation field, H_{int} becomes

$$H_{\text{int}} = -\frac{\gamma_g\hbar}{2c}\sqrt{\frac{\hbar\omega}{2\varepsilon_0 V}}(I_- a + I_+ a^+) + \frac{\gamma_g\hbar}{2c}\sqrt{\frac{\hbar\omega}{2\varepsilon_0 V}}(I_+ a + I_- a^+) \tag{14}$$

where I_+ and I_- are the usual nuclear spin raising and lowering operators in the primed axis system. When the lowest energy corresponds to the state with quantum number $1/2$, only the first two terms couple the states. The other two correspond to virtual (energy non-conservation) processes. It is this case that will be considered in the following (e.g. ground state of ^{57}Fe). If, on the contrary, the lowest energy were the state characterized by $-1/2$, only the last two terms would couple the states and the first two would correspond to virtual processes.

The total Hamiltonian of the global system is then

$$H = H_0 + H_{\text{int}} \tag{15}$$

where H_{int} is now given by the first two terms of expression (14). Evaluating the matrix in the case 1 basis system gives

$$H_g = \begin{pmatrix} E_{1g} & g\sqrt{n} \\ g\sqrt{n} & E_{2g} \end{pmatrix} \tag{16}$$

where

$$g = -\frac{\gamma_g \bar{h}}{2c}\sqrt{\frac{\bar{h}\omega}{2\varepsilon_0 V}}. \tag{17}$$

The eigenvalues of H_g can be found after a straightforward calculation. They are

$$\lambda_\pm = \frac{E_{1g}+E_{2g}}{2} \pm \frac{1}{2}\sqrt{(E_{2g}-E_{1g})^2 + 4g^2 n} = n\bar{h}\omega \pm \frac{1}{2}\sqrt{\bar{h}^2\Delta\omega^2 + 4g^2 n}. \tag{18}$$

3.1.2. Case 2. In a similar fashion we now treat the two-dimensional vector space arising from case 2. The energy eigenvalues in the absence of rf coupling are

$$\begin{aligned} &|\varphi_2'\rangle \text{ has energy } E'_{1g} = -\tfrac{1}{2}\gamma_g \bar{h} B_0 + \bar{h}\omega(n+\tfrac{3}{2}) \\ &|\varphi_1'\rangle \text{ has energy } E'_{2g} = \tfrac{1}{2}\gamma_g \bar{h} B_0 + \bar{h}\omega(n+\tfrac{1}{2}). \end{aligned} \tag{19}$$

Following the same procedure as above gives

$$H'_g = \begin{pmatrix} E'_{1g} & g\sqrt{n+1} \\ g\sqrt{n+1} & E'_{2g} \end{pmatrix}. \tag{20}$$

Again the eigenvalues of H'_g can be found. They are

$$\begin{aligned} \lambda'_\pm &= \frac{E'_{1g}+E'_{2g}}{2} \pm \frac{1}{2}\sqrt{(E'_{2g}-E'_{1g})^2 + 4g^2(n+1)} \\ &= (n+1)\bar{h}\omega \pm \frac{1}{2}\sqrt{\bar{h}^2\Delta\omega^2 + 4g^2(n+1)}. \end{aligned} \tag{21}$$

It is not difficult to show that

$$4g^2 n = \frac{1}{2}\frac{B_{rf}^2}{B_0^2}\bar{h}^2\omega_g^2 \tag{22}$$

where B_{rf} is the magnitude of the magnetic flux density in the rf radiation. Also it is not difficult to show that under normal conditions $n \gg 1$. Using these considerations, the energy eigenvalues are shown in figure 1. Figure 1 shows the energies E_{1g}, E_{2g}, E'_{1g} and E'_{2g}, the eigenvalues in the absence of the rf coupling, as a function of the ratio of the rf frequency (ω) to the resonant frequency (ω_g). The actual energies have been redefined by subtracting everywhere $n\bar{h}\omega$. These are the four straight lines in figure 1 (only one of them, E_{2g}, has a negative slope because of the presence of $-\frac{1}{2}\bar{h}\omega$). The eigenvalues $\lambda_\pm$ and $\lambda'_\pm$ (also 'renormalized' by subtraction of $n\bar{h}\omega$), which are a consequence of the rf coupling, are also shown in figure 1 as a function of the same ratio. The magnitude of the rf magnetic field is taken as 8 tesla and the magnitude of the Zeeman magnetic field is taken as 33 tesla. There are several observations that one should make from this figure. Notice that at $\omega = \omega_g$, the resonant frequency, $E_{1g} = E_{2g}$ and $E'_{1g} = E'_{2g}$. Furthermore we note that

$$\begin{aligned} &\lambda_- \text{ is close to } E_{1g} \text{ when } \omega \ll \omega_g \qquad \left(\lim_{\omega\to 0}\lambda_- = E_{1g}\right) \\ &\lambda_- \text{ is close to } E_{2g} \text{ when } \omega \gg \omega_g \qquad \left(\lim_{\omega\to \infty}\lambda_- = E_{2g}\right) \end{aligned} \tag{23}$$

and

$$\begin{aligned} &\lambda_+ \text{ is close to } E_{2g} \text{ when } \omega \ll \omega_g \qquad \left(\lim_{\omega\to 0}\lambda_+ = E_{2g}\right) \\ &\lambda_+ \text{ is close to } E_{1g} \text{ when } \omega \gg \omega_g \qquad \left(\lim_{\omega\to \infty}\lambda_+ = E_{1g}\right). \end{aligned} \tag{24}$$

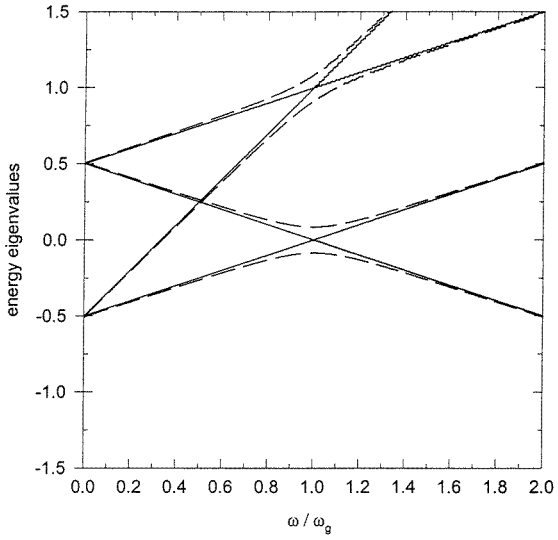

Figure 1. Eigenvalues of the dressed and undressed nuclear spin 1/2 Zeeman-split ground state corresponding to the presence of n and $n+1$ photons. $n\bar{h}\omega$ has been subtracted from all energies. The eigenvalues are plotted as a function of the ratio of the angular frequency ω of the transverse applied rf field to the resonant ground-state Zeeman-split frequency ω_g. The Zeeman magnetic field B_0 is taken equal to 33 tesla and the magnitude of the rf magnetic flux density B_{rf} is equal to 8 tesla. The order of the energy eigenvalues can be identified by considering the figure at the frequency ratio of about 0.8. Starting from the top curve and going down, the curves correspond to λ'_+, E'_{2g}, E'_{1g}, λ'_-, λ_+, E_{2g}, E_{1g} and λ_-.

This means that at resonance there is a twofold degeneracy, in the absence of the rf coupling, which is removed by the interaction. Of course a similar situation exists for $\lambda'_\pm$ as shown in figure 1. Let us introduce the splitting parameters Δ and Δ' corresponding to the energy separation between each pair of dashed lines in figure 1, where

$$\begin{aligned}\Delta &= \sqrt{\bar{h}^2\Delta\omega^2 + 4g^2n} = \sqrt{\bar{h}^2\Delta\omega^2 + \frac{1}{2}\frac{B_{rf}^2}{B_0^2}\bar{h}^2\omega_g^2} \\ \Delta' &= \sqrt{\bar{h}^2\Delta\omega^2 + 4g^2(n+1)} = \sqrt{\bar{h}^2\Delta\omega^2 + \frac{1}{2}\frac{B_{rf}^2}{B_0^2}\bar{h}^2\omega_g^2 + \frac{1}{2}\frac{B_{rf}^2}{B_0^2 n}\bar{h}^2\omega_g^2}.\end{aligned} \tag{25}$$

Then (18) and (21) become

$$\begin{aligned}\lambda_\pm &= n\bar{h}\omega \pm \tfrac{1}{2}\Delta \\ \lambda'_\pm &= (n+1)\bar{h}\omega \pm \tfrac{1}{2}\Delta'.\end{aligned} \tag{26}$$

At resonance one has

$$\begin{aligned}\Delta &= 2g\sqrt{n} = \sqrt{\frac{1}{2}\frac{B_{rf}^2}{B_0^2}\bar{h}^2\omega_g^2} \\ \Delta' &= 2g\sqrt{n+1} = \sqrt{\frac{1}{2}\frac{B_{rf}^2}{B_0^2}\bar{h}^2\omega_g^2 + \frac{1}{2}\frac{B_{rf}^2}{B_0^2 n}\bar{h}^2\omega_g^2}.\end{aligned} \tag{27}$$

For large n, $\Delta \approx \Delta'$. The condition of large n is always realized, as mentioned above.

Due to the interaction of the nuclei with the rf field the quasi-degeneracy of the energy is lifted. The splitting parameter Δ can be interpreted as a Rabi splitting, as will be discussed below in section 3.3.

In the next section we will find the eigenstates of the system in the presence of rf coupling. For the situation discussed in this paper the excited nuclear states are not coupled by the rf-radiation field (far off-resonance condition), while the nuclear ground-state sublevels are coupled strongly by the rf-radiation field.

3.2. Eigenstates

In order to calculate the possible transition energies we need to find the eigenstates belonging to $\lambda_\pm$ and $\lambda'_\pm$. A straightforward calculation leads to the following normalized eigenvectors belonging to the eigenvalues λ_- and λ_+.

$$|\psi_-\rangle = -\sin\frac{\alpha}{2}|\varphi_1\rangle + \cos\frac{\alpha}{2}|\varphi_2\rangle$$

and

$$|\psi_+\rangle = \cos\frac{\alpha}{2}|\varphi_1\rangle + \sin\frac{\alpha}{2}|\varphi_2\rangle \tag{28}$$

where α, the 'mixing angle', is defined by

$$\tan\alpha = \frac{2g\sqrt{n}}{\hbar\omega - \gamma_g\hbar B_0} = \frac{2g\sqrt{n}}{\hbar\Delta\omega} = \frac{1}{\sqrt{2}}\frac{B_{rf}}{B_0}\frac{\omega_g}{\Delta\omega} \qquad 0 < \alpha \leqslant \pi. \tag{29}$$

Notice that at resonance $\alpha = \pi/2$.

Similarly the normalized eigenvectors belonging to λ'_- and λ'_+ are respectively

$$|\psi'_-\rangle = -\sin\frac{\alpha'}{2}|\varphi'_2\rangle + \cos\frac{\alpha'}{2}|\varphi'_1\rangle$$

and

$$|\psi'_+\rangle = \cos\frac{\alpha'}{2}|\varphi'_2\rangle + \sin\frac{\alpha'}{2}|\varphi'_1\rangle \tag{30}$$

where the mixing angle α' is defined by

$$\tan\alpha' = \frac{2g\sqrt{n+1}}{\hbar\omega - \gamma_g\hbar B_0} = \frac{2g\sqrt{n+1}}{\hbar\Delta\omega} \approx \frac{1}{\sqrt{2}}\frac{B_{rf}}{B_0}\frac{\omega_g}{\Delta\omega} \qquad 0 < \alpha' \leqslant \pi. \tag{31}$$

Equation (31) shows that for large n, $\alpha \approx \alpha'$.

3.3. Time dependence

In this section we will treat the time dependence of the nuclear ground states which are coupled by the rf field. This is not difficult to do because of the dressed-state formulation. We will consider only the case 1 condition, since the case 2 situation can be treated in essentially the same way.

Assume that at time $t = 0$ the system is in the state $|\varphi_1\rangle$. This state is not an eigenstate of the system when there is rf coupling. However, it is easy to invert (28) to obtain

$$|\varphi_1\rangle = \cos\frac{\alpha}{2}|\psi_+\rangle - \sin\frac{\alpha}{2}|\psi_-\rangle$$

and

$$|\varphi_2\rangle = \sin\frac{\alpha}{2}|\psi_+\rangle + \cos\frac{\alpha}{2}|\psi_-\rangle. \tag{32}$$

Thus, if we assume that the resonance condition is satisfied, we can write

$$|\varphi_1\rangle = \frac{1}{\sqrt{2}}|\psi_+(t=0)\rangle - \frac{1}{\sqrt{2}}|\psi_-(t=0)\rangle. \tag{33}$$

The time evolution of this state is easily determined because the eigenstates of the system evolve in time according to the usual time evolution operator. Thus we can express the time evolution of the initial state as

$$|\varphi_1(t)\rangle = \frac{1}{\sqrt{2}}\,\mathrm{e}^{-\mathrm{i}\lambda_+ t/\hbar}|\psi_+(t=0)\rangle - \frac{1}{\sqrt{2}}\,\mathrm{e}^{-\mathrm{i}\lambda_- t/\hbar}|\psi_-(t=0)\rangle. \tag{34}$$

The time-dependent probability for finding the system in its original state is obtained by finding that

$$|\langle\varphi_1 \mid \varphi_1(t)\rangle|^2 = \cos^2\left(\frac{\Delta t}{2\hbar}\right) \tag{35}$$

where Δ is the energy separation of the two energy levels evaluated on resonance. This shows the familiar Rabi behaviour in which the system is initially in a particular state, but as a function of time oscillates between the initial state and another one, in this case $|\varphi_2\rangle$. Similarly one can show the other familiar result

$$|\langle\varphi_2 \mid \varphi_1(t)\rangle|^2 = \sin^2\left(\frac{\Delta t}{2\hbar}\right). \tag{36}$$

Although these results are for the on-resonance condition, it is clear that the formalism is capable of handling the most general cases.

4. Spontaneous emission

4.1. Energies of the emitted photons

As already mentioned above we suppose that the excited-state nuclear Zeeman sublevels are not coupled by the rf-radiation field. This is, for most cases, a reasonable assumption since the hyperfine splitting in the excited state is generally very different from that in the ground state. Thus, since we are considering the case of resonance in the ground state, we assume no rf coupling in the excited states. The energies of the system formed by the first-excited nuclear states and the rf field, for the far off-resonance condition, are simply

$$E_{e,m_e} = E_0 - \gamma_e\hbar B_0 m'_e + \hbar\omega(n + \tfrac{1}{2}) \tag{37}$$

with $-3/2 \leqslant m'_e \leqslant 3/2$. The corresponding eigenstates are direct product states of $|3/2, m'_e\rangle$ with the eigenstates of the radiation field, namely $|n\rangle$.The transition energies between these states and the ground states are listed in table 1. Next, we need to calculate the transition probabilities for each transition.

4.2. Transition probabilities

We will now consider the magnetic dipole (M1) transition which applies to the 14.4 keV transition in ^{57}Fe. The interaction describing spontaneous emission through an M1-transition is given by a complicated expression [10], which can be reduced to

$$H_{sp.em.} = \frac{\mathrm{i}}{c}\boldsymbol{\mu}\cdot\sum_{l,\sigma}\sqrt{\frac{\hbar\omega_l}{2\varepsilon_0 V}}\boldsymbol{u}_l(a_{l,\sigma}\,\mathrm{e}^{\mathrm{i}\boldsymbol{l}\cdot\boldsymbol{r}} - a^+_{l,\sigma}\,\mathrm{e}^{-\mathrm{i}\boldsymbol{l}\cdot\boldsymbol{r}}). \tag{38}$$

Table 1. Energies and relative transition probabilities of photons emitted by an ensemble of nuclei (in a static constant hyperfine magnetic field) having an excited state 3/2 and a ground state 1/2 with the ground-state Zeeman levels coupled by a transverse rf field for an arbitrary coupling strength and for any photon emission direction in the plane perpendicular to the applied rf magnetic flux density.

Transitions	Energies	Relative transition probabilities
$E_1 = E_{e,-3/2} - \lambda_-$	$E_0 - \frac{3\lvert\gamma_e\rvert\overline{h}B_0}{2} + \frac{\overline{h}\omega}{2} + \frac{\Delta}{2}$	0
$E_2 = E_{e,-1/2} - \lambda_-$	$E_0 - \frac{\lvert\gamma_e\rvert\overline{h}B_0}{2} + \frac{\overline{h}\omega}{2} + \frac{\Delta}{2}$	$\sin^2\frac{\alpha}{2}\left(\sin^4\frac{\beta}{2} + \cos^4\frac{\beta}{2}\right)$
$E_3 = E_{e,+1/2} - \lambda_-$	$E_0 + \frac{\lvert\gamma_e\rvert\overline{h}B_0}{2} + \frac{\overline{h}\omega}{2} + \frac{\Delta}{2}$	$8\sin^2\frac{\alpha}{2}\sin^2\frac{\beta}{2}\cos^2\frac{\beta}{2}$
$E_4 = E_{e,+3/2} - \lambda_-$	$E_0 + \frac{3\lvert\gamma_e\rvert\overline{h}B_0}{2} + \frac{\overline{h}\omega}{2} + \frac{\Delta}{2}$	$3\sin^2\frac{\alpha}{2}\left(\sin^4\frac{\beta}{2} + \cos^4\frac{\beta}{2}\right)$
$E_5 = E_{e,-3/2} - \lambda_+$	$E_0 - \frac{3\lvert\gamma_e\rvert\overline{h}B_0}{2} + \frac{\overline{h}\omega}{2} - \frac{\Delta}{2}$	0
$E_6 = E_{e,-1/2} - \lambda_+$	$E_0 - \frac{\lvert\gamma_e\rvert\overline{h}B_0}{2} + \frac{\overline{h}\omega}{2} - \frac{\Delta}{2}$	$\cos^2\frac{\alpha}{2}\left(\sin^4\frac{\beta}{2} + \cos^4\frac{\beta}{2}\right)$
$E_7 = E_{e,+1/2} - \lambda_+$	$E_0 + \frac{\lvert\gamma_e\rvert\overline{h}B_0}{2} + \frac{\overline{h}\omega}{2} - \frac{\Delta}{2}$	$8\cos^2\frac{\alpha}{2}\sin^2\frac{\beta}{2}\cos^2\frac{\beta}{2}$
$E_8 = E_{e,+3/2} - \lambda_+$	$E_0 + \frac{3\lvert\gamma_e\rvert\overline{h}B_0}{2} + \frac{\overline{h}\omega}{2} - \frac{\Delta}{2}$	$3\cos^2\frac{\alpha}{2}\left(\sin^4\frac{\beta}{2} + \cos^4\frac{\beta}{2}\right)$
$E_9 = E_{e,-3/2} - \lambda'_-$	$E_0 - \frac{3\lvert\gamma_e\rvert\overline{h}B_0}{2} - \frac{\overline{h}\omega}{2} + \frac{\Delta}{2}$	$3\cos^2\frac{\alpha}{2}\left(\sin^4\frac{\beta}{2} + \cos^4\frac{\beta}{2}\right)$
$E_{10} = E_{e,-1/2} - \lambda'_-$	$E_0 - \frac{\lvert\gamma_e\rvert\overline{h}B_0}{2} - \frac{\overline{h}\omega}{2} + \frac{\Delta}{2}$	$8\cos^2\frac{\alpha}{2}\sin^2\frac{\beta}{2}\cos^2\frac{\beta}{2}$
$E_{11} = E_{e,+1/2} - \lambda'_-$	$E_0 + \frac{\lvert\gamma_e\rvert\overline{h}B_0}{2} - \frac{\overline{h}\omega}{2} + \frac{\Delta}{2}$	$\cos^2\frac{\alpha}{2}\left(\sin^4\frac{\beta}{2} + \cos^4\frac{\beta}{2}\right)$
$E_{12} = E_{e,+3/2} - \lambda'_-$	$E_0 + \frac{3\lvert\gamma_e\rvert\overline{h}B_0}{2} - \frac{\overline{h}\omega}{2} + \frac{\Delta}{2}$	0
$E_{13} = E_{e,-3/2} - \lambda'_+$	$E_0 - \frac{3\lvert\gamma_e\rvert\overline{h}B_0}{2} - \frac{\overline{h}\omega}{2} - \frac{\Delta}{2}$	$3\sin^2\frac{\alpha}{2}\left(\sin^4\frac{\beta}{2}\cos^4\frac{\beta}{2}\right)$
$E_{14} = E_{e,-1/2} - \lambda'_+$	$E_0 - \frac{\lvert\gamma_e\rvert\overline{h}B_0}{2} - \frac{\overline{h}\omega}{2} - \frac{\Delta}{2}$	$8\sin^2\frac{\alpha}{2}\sin^2\frac{\beta}{2}\cos^2\frac{\beta}{2}$
$E_{15} = E_{e,+1/2} - \lambda'_+$	$E_0 + \frac{\lvert\gamma_e\rvert\overline{h}B_0}{2} - \frac{\overline{h}\omega}{2} - \frac{\Delta}{2}$	$\sin^2\frac{\alpha}{2}\left(\sin^4\frac{\beta}{2} + \cos^4\frac{\beta}{2}\right)$
$E_{16} = E_{e,+3/2} - \lambda'_+$	$E_0 + \frac{3\lvert\gamma_e\rvert\overline{h}B_0}{2} - \frac{\overline{h}\omega}{2} - \frac{\Delta}{2}$	0

$\boldsymbol{\mu}$ is the 'real' magnetic dipole operator which contains, in principle, the properties of all nucleons composing the nucleus. However we do not need the exact expression, since the magnetic moments and spins of the nuclear states in question are already known. The term with the summation sign is proportional to the virtual magnetic flux density due to the vacuum fluctuations. The $a_{\boldsymbol{l},\sigma}$ and $a^+_{\boldsymbol{l},\sigma}$ are respectively the annihilation and creation operators relative to the virtual field photon with wave vector $\boldsymbol{l}$ and polarization σ. The other quantities in (38) are standard in the theory of quantized fields. The only thing that we have to realize here is that, due to the specific form of $H_{sp.em.}$, the number of real rf photons cannot change by the process of spontaneous emission. This means that when the global system emits a gamma ray, going from a $|\psi_e\rangle$ to one of its ground states given by

eigenvectors $|\psi_-\rangle$, $|\psi_+\rangle$, $|\psi'_-\rangle$ and $|\psi'_+\rangle$ (see (28) and (30)), one only has to consider the part of these states containing $|n\rangle$. Furthermore there is a nuclear-state selection rule which, for a magnetic dipole transition, is $\Delta m = m_g - m_e = 0, \pm 1$.

We will now introduce another z-axis which will be our quantization axis for our final calculations. This z-axis is in the direction of the recorded gamma rays determined by the position of the detector relative to the radioactive source. We assume that the z-axis is also perpendicular to the y'-axis. This is not essential. However, if this condition is not imposed the resulting expressions become quite cumbersome. The direction of the static Zeeman magnetic field, as noted above, is along the z'-axis which, in general, makes an angle β with respect to the z-axis. One can easily go from the z'-axis system to the z-axis system by a rotation about the y'-axis through an angle β. With respect to this new z-axis system the nuclear ground- and excited-state levels are no longer pure 'm' states. However the states with respect to this new z-axis can be easily found by using the familiar rotation matrices [10], usually written as $d^I_{m'm}$. The 'old' states can be expressed in terms of the 'new' states by

$$|I, m'\rangle = \sum_m |I, m\rangle d^I_{m,m'}(\beta) \tag{39}$$

where for our nuclear ground states we have

$$d^{1/2} = \begin{pmatrix} \cos\dfrac{\beta}{2} & \sin\dfrac{\beta}{2} \\ -\sin\dfrac{\beta}{2} & \cos\dfrac{\beta}{2} \end{pmatrix}. \tag{40}$$

The two ground states can thus be written as

$$\begin{aligned} |\tfrac{1}{2}, \tfrac{1}{2}'\rangle &= \cos\frac{\beta}{2}|\tfrac{1}{2}, \tfrac{1}{2}\rangle - \sin\frac{\beta}{2}|\tfrac{1}{2}, -\tfrac{1}{2}\rangle \\ |\tfrac{1}{2}, -\tfrac{1}{2}'\rangle &= \sin\frac{\beta}{2}|\tfrac{1}{2}, \tfrac{1}{2}\rangle + \cos\frac{\beta}{2}|\tfrac{1}{2}, -\tfrac{1}{2}\rangle. \end{aligned} \tag{41}$$

Next we need to find the form of the excited nuclear eigenstates in the z-axis system. This can, of course, be done in a similar fashion. The rotation matrix for this case is

$$d^{3/2} = \begin{Bmatrix} \cos^3\dfrac{\beta}{2} & \sqrt{3}\cos^2\dfrac{\beta}{2}\sin\dfrac{\beta}{2} \\ -\sqrt{3}\cos^2\dfrac{\beta}{2}\sin\dfrac{\beta}{2} & \cos\dfrac{\beta}{2}\left(3\cos^2\dfrac{\beta}{2} - 2\right) \\ \sqrt{3}\cos\dfrac{\beta}{2}\sin^2\dfrac{\beta}{2} & \sin\dfrac{\beta}{2}\left(3\sin^2\dfrac{\beta}{2} - 2\right) \\ -\sin^3\dfrac{\beta}{2} & \sqrt{3}\cos\dfrac{\beta}{2}\sin^2\dfrac{\beta}{2} \end{Bmatrix}$$

$$\begin{Bmatrix} \sqrt{3}\cos\dfrac{\beta}{2}\sin^2\dfrac{\beta}{2} & \sin^3\dfrac{\beta}{2} \\ -\sin\dfrac{\beta}{2}\left(3\sin^2\dfrac{\beta}{2} - 2\right) & \sqrt{3}\cos\dfrac{\beta}{2}\sin^2\dfrac{\beta}{2} \\ \cos\dfrac{\beta}{2}\left(3\cos^2\dfrac{\beta}{2} - 2\right) & \sqrt{3}\cos^2\dfrac{\beta}{2}\sin\dfrac{\beta}{2} \\ -\sqrt{3}\cos^2\dfrac{\beta}{2}\sin\dfrac{\beta}{2} & \cos^3\dfrac{\beta}{2} \end{Bmatrix}. \tag{42}$$

The first-excited nuclear eigenstates can be written in the z-axis system as

$$|3/2, m'_e\rangle = \sum_{m_e} |3/2, m_e\rangle d^{3/2}_{m_e,m'_e}(\beta) \tag{43}$$

where the needed matrix elements are given in (42).

In order to calculate the transition probabilities we need the eigenfunctions for the global system. Since we assume that we are far off resonance for the nuclear excited states, $I_e = 3/2$, these global eigenfunctions can be expressed easily in the z-axis system as

$$|\psi_e(m'_e)\rangle = \sum_{m_e} |3/2, m_e\rangle d^{3/2}_{m_e,m'_e} \otimes |n\rangle. \tag{44}$$

Writing these out explicitly, we find

$$|\psi_e(3/2)'\rangle = \begin{bmatrix} \cos^3\frac{\beta}{2}|3/2, 3/2\rangle - \sqrt{3}\cos^2\frac{\beta}{2}\sin\frac{\beta}{2}|3/2, 1/2\rangle \\ +\sqrt{3}\cos\frac{\beta}{2}\sin^2\frac{\beta}{2}|3/2, -1/2\rangle - \sin^3\frac{\beta}{2}|3/2, -3/2\rangle \end{bmatrix} \otimes |n\rangle$$

$$|\psi_e(1/2)'\rangle = \begin{bmatrix} \sqrt{3}\cos^2\frac{\beta}{2}\sin\frac{\beta}{2}|3/2, 3/2\rangle + \cos\frac{\beta}{2}\left(3\cos^2\frac{\beta}{2} - 2\right)|3/2, 1/2\rangle \\ +\sin\frac{\beta}{2}\left(3\sin^2\frac{\beta}{2} - 2\right)|3/2, -1/2\rangle + \sqrt{3}\cos\frac{\beta}{2}\sin^2\frac{\beta}{2}|3/2, -3/2\rangle \end{bmatrix} \otimes |n\rangle$$

$$|\psi_e(-1/2)'\rangle = \begin{bmatrix} \sqrt{3}\cos\frac{\beta}{2}\sin^2\frac{\beta}{2}|3/2, 3/2\rangle - \sin\frac{\beta}{2}\left(3\sin^2\frac{\beta}{2} - 2\right)|3/2, 1/2\rangle \\ +\cos\frac{\beta}{2}\left(3\cos^2\frac{\beta}{2} - 2\right)|3/2, -1/2\rangle - \sqrt{3}\cos^2\frac{\beta}{2}\sin\frac{\beta}{2}|3/2, -3/2\rangle \end{bmatrix} \otimes |n\rangle$$

$$|\psi_e(-3/2)'\rangle = \begin{bmatrix} \sin^3\frac{\beta}{2}|3/2, 3/2\rangle + \sqrt{3}\cos\frac{\beta}{2}\sin^2\frac{\beta}{2}|3/2, 1/2\rangle \\ +\sqrt{3}\cos^2\frac{\beta}{2}\sin\frac{\beta}{2}|3/2, -1/2\rangle + \cos^3\frac{\beta}{2}|3/2, -3/2\rangle \end{bmatrix} \otimes |n\rangle. \tag{45}$$

Now the eigenfunctions for the rf-coupled global system ground-state levels, in the z-axis system, can be obtained by combining (28), (30) and (41). The results, written out

explicitly, are

$$
\begin{aligned}
|\psi_{g,-}\rangle &= -\sin\frac{\alpha}{2}\left(\cos\frac{\beta}{2}\left|\frac{1}{2},\frac{1}{2}\right\rangle - \sin\frac{\beta}{2}\left|\frac{1}{2},-\frac{1}{2}\right\rangle\right)\otimes|n\rangle \\
&\quad + \cos\frac{\alpha}{2}\left(\sin\frac{\beta}{2}\left|\frac{1}{2},\frac{1}{2}\right\rangle + \cos\frac{\beta}{2}\left|\frac{1}{2},-\frac{1}{2}\right\rangle\right)\otimes|n-1\rangle \\
|\psi_{g,+}\rangle &= \cos\frac{\alpha}{2}\left(\cos\frac{\beta}{2}\left|\frac{1}{2},\frac{1}{2}\right\rangle - \sin\frac{\beta}{2}\left|\frac{1}{2},-\frac{1}{2}\right\rangle\right)\otimes|n\rangle \\
&\quad + \sin\frac{\alpha}{2}\left(\sin\frac{\beta}{2}\left|\frac{1}{2},\frac{1}{2}\right\rangle + \cos\frac{\beta}{2}\left|\frac{1}{2},-\frac{1}{2}\right\rangle\right)\otimes|n-1\rangle \\
|\psi'_{g,-}\rangle &= -\sin\frac{\alpha'}{2}\left(\cos\frac{\beta}{2}\left|\frac{1}{2},\frac{1}{2}\right\rangle - \sin\frac{\beta}{2}\left|\frac{1}{2},-\frac{1}{2}\right\rangle\right)\otimes|n+1\rangle \\
&\quad + \cos\frac{\alpha'}{2}\left(\sin\frac{\beta}{2}\left|\frac{1}{2},\frac{1}{2}\right\rangle + \cos\frac{\beta}{2}\left|\frac{1}{2},-\frac{1}{2}\right\rangle\right)\otimes|n\rangle \\
|\psi'_{g,+}\rangle &= \cos\frac{\alpha'}{2}\left(\cos\frac{\beta}{2}\left|\frac{1}{2},\frac{1}{2}\right\rangle - \sin\frac{\beta}{2}\left|\frac{1}{2},-\frac{1}{2}\right\rangle\right)\otimes|n+1\rangle \\
&\quad + \sin\frac{\alpha'}{2}\left(\sin\frac{\beta}{2}\left|\frac{1}{2},\frac{1}{2}\right\rangle + \cos\frac{\beta}{2}\left|\frac{1}{2},-\frac{1}{2}\right\rangle\right)\otimes|n\rangle
\end{aligned}
\tag{46}
$$

where we have explicitly added the subscript g to emphasize the nuclear ground states. To avoid any confusion it should be mentioned at this stage that the prime at the left-hand side of the last two expressions of (46) refers to the states corresponding to the eigenvalues $\lambda'_{\pm}$, given by expression (21).

The matrix element describing the spontaneous emission from an initial state $|\psi_i\rangle$ to a final state $|\psi_f\rangle$ is generally written as

$$M_{fi} = \langle\psi_f|H_{sp.em.}|\psi_i\rangle \tag{47}$$

where $H_{sp.em.}$ is the operator describing the transition. This expression takes on a simplified form for a magnetic dipole transition between two eigenstates in the z-axis system. One can write [11, 12] for the amplitude and polarization of the emitted phonon

$$A_{I_f m_f; I_i m_i} = C(I_f, m_f; 1, M|I_i m_i)\boldsymbol{X}_{1,M} \tag{48}$$

where C is an overall constant containing amongst others the nuclear reduced matrix element, $(I_f, m_f; 1, M \mid I_i m_i)$ is the Clebsch–Gordan coefficient and $\boldsymbol{X}_{1,M}$ is the vector spherical harmonic. The vector spherical harmonics $\boldsymbol{X}_{1,M}$ $(M = 1, 0, -1)$, representing the photon in the final state of the system, are appropriate for magnetic dipole radiation since they describe not only the angular distribution but also the polarization of the emitted photons.

In our case $|\psi_i\rangle$ and $|\psi_f\rangle$ are linear combinations of eigenstates of the z-component of angular momentum. So evaluating (47) leads to a sum of matrix-element terms where each term is of the form given by (48).

The vector spherical harmonics for dipole radiation are

$$\begin{aligned} \boldsymbol{X}_{1,\pm1} &= \sqrt{\frac{3}{16\pi}}(\mathrm{e}^{\pm\mathrm{i}\phi}\boldsymbol{a}_\theta \pm \mathrm{i}\cos\theta\,\mathrm{e}^{\pm\mathrm{i}\phi}\boldsymbol{a}_\phi) \\ \boldsymbol{X}_{1,0} &= \mathrm{i}\sqrt{\frac{3}{8\pi}}\sin\theta\boldsymbol{a}_\phi \end{aligned} \tag{49}$$

where $\boldsymbol{a}_\theta$ and $\boldsymbol{a}_\phi$ are the usual unit vectors in spherical coordinates θ, ϕ. From conservation of angular momentum the appropriate vector spherical harmonic is associated with the change in the nuclear spin projection quantum number. In the z-direction $\theta = 0$ and $\phi = 0$, so that only two vector spherical harmonics are non-zero and one has

$$\begin{aligned} \boldsymbol{X}_{1,\pm1} &= \sqrt{\frac{3}{16\pi}}(\boldsymbol{u}_x \pm \mathrm{i}\boldsymbol{u}_y) \\ \boldsymbol{X}_{1,0} &= \boldsymbol{0}. \end{aligned} \tag{50}$$

These correspond to photons having right- and left-handed circular polarization, i.e. -1 and $+1$ helicities. The nuclear transitions that produce radiation for this case correspond to $\Delta m = \pm 1$ only. (Also note that $\boldsymbol{X}_{1,1} \cdot \boldsymbol{X}^*_{1,-1} = 0$.) With the aid of (45)–(50), the transition matrix elements and hence the transition probabilities can be calculated. They are given in table 1. There are 16 different energies to which have been assigned numbers from 1 to 16 in the first column of table 1. Figure 2 gives the complete energy spectrum as well as the 12 possible transitions consistent with the M1 selection rules. From table 1, the transition probabilities depend on the angles α and β. The angle α is determined by the coupling strength of the interaction between the nuclei and the rf field as seen in (29) and (31). This coupling strength depends on the ratio of the magnitude of the rf magnetic flux density to that of the static Zeeman field as well as the detuning factor $\Delta\omega$. The angle β is determined by the direction of the Zeeman magnetic field, given by z', relative to the photon emission direction taken as along the z-axis.

From table 1 it can be verified easily that one obtains the well known emission spectra under familiar cases. For example, consider the case when there is no rf coupling ($\alpha = 0$) and the photon is emitted along the direction of the Zeeman magnetic field ($\beta = 0$). It is easy to see that the six emission lines, ordered in terms of increasing energy, have intensities of 3, 0, 1, 1, 0, 3. Similarly when there is no rf coupling and the photon emission direction is at 90° with respect to the Zeeman magnetic field the emission intensities are 3, 4, 1, 1, 4, 3. Figure 3 shows the source emission spectrum under these conditions assuming B_0 equals 33 tesla.

Under the same conditions as mentioned above, consider the case when the rf-resonance condition is satisfied, i.e. $\alpha = \pi/2$. Now each emission line is split into two. Thus, for photon emission along the Zeeman magnetic field, the emission spectrum now has a total of eight peaks composed of four closely spaced pairs of peaks. Similarly, when the photon direction is at 90° with respect to the Zeeman magnetic field the emission spectrum consists of 12 peaks composed of six closely spaced pairs of peaks. Figure 4 shows the source emission spectrum under these two conditions assuming B_0 equals 33 tesla and the strength of the rf coupling is such that $\Delta = 4\Gamma$, where Γ is the natural linewidth of the first-excited nuclear state.

4.3. Simulated Mössbauer spectra

The complete information about the energies and relative line intensities of radiation emitted by an ensemble of ^{57}Fe nuclei in a Zeeman magnetic field when there is an additional

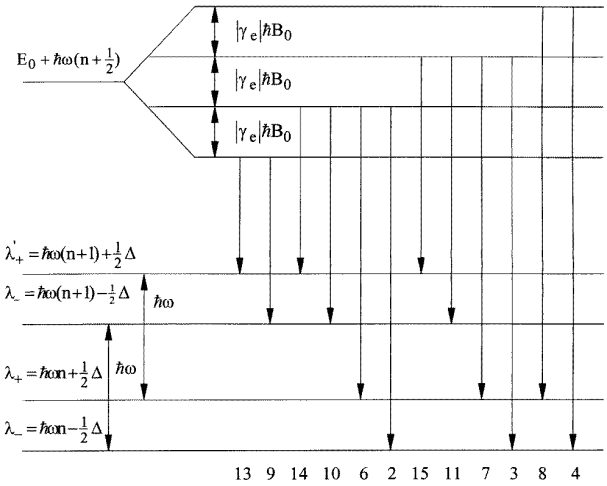

Figure 2. Energy scheme of an ensemble of dressed nuclei (ground-state dressing by an rf field) of an ensemble of nuclei in a magnetic field having an excited-state spin $= 3/2$ and a ground-state spin $= 1/2$. The 12 possible transitions are indicated. The numbers at the bottom correspond to the same energy numbering as in the first column of table 1.

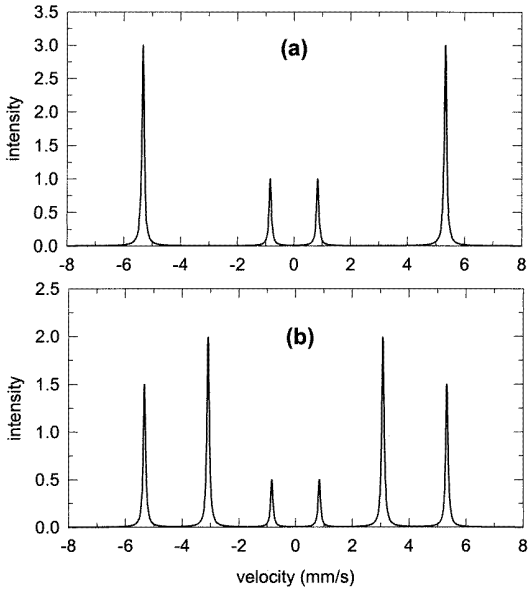

Figure 3. Gamma-ray emission spectrum from a Zeeman-split ^{57}Fe source when the photon direction is parallel to the Zeeman field (a) and perpendicular to the Zeeman field (b) in the absence of rf coupling. The energy of the photons is relative to the field-free energy separation between the ground- and first-excited-state nuclear levels E_0, and in units of the natural linewidth Γ. (The Zeeman magnetic field B_0 is taken as 33 tesla.)

interaction due to a transverse rf field, which couples the ground state, is contained in table 1. These results apply for all angles of the internal constant Zeeman hyperfine magnetic field (B_0) lying in the plane perpendicular to the magnetic flux density $\boldsymbol{B}_{rf}$ of the rf field and for all coupling strengths arising from the magnitude of the rf magnetic flux density.

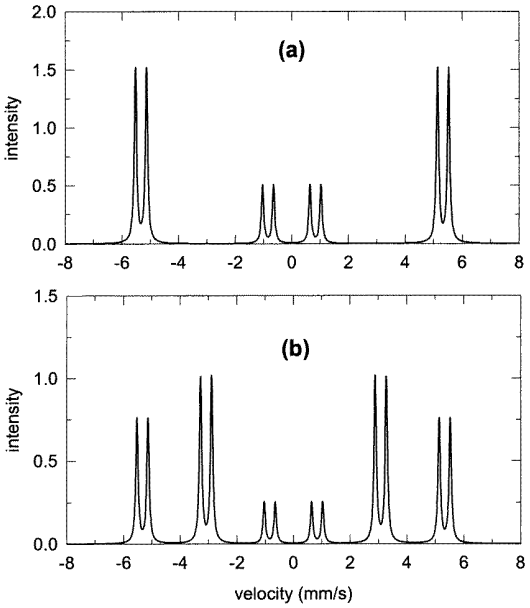

Figure 4. Gamma-ray emission spectrum from a Zeeman-split ^{57}Fe source when the photon direction is parallel to the Zeeman field (a) and perpendicular to the Zeeman field (b) in the presence of rf coupling in the ground state on resonance. The strength of the rf coupling is taken to be $\Delta = 4\Gamma$. As the strength of the rf coupling increases, the energy separation of the doublets would increase. The energy of the photons is relative to the field-free energy separation between the ground- and first-excited-state nuclear levels E_0, and in units of the natural linewidth Γ. (The Zeeman magnetic field B_0 is taken as 33 tesla.)

The separation in energy of the doublet peaks is given by the splitting parameters Δ and Δ' which depend on the coupling strength between the rf field and the nucleus, see (25). In order to observe these spectra using the Mössbauer effect, splittings on the order of, or larger than, the natural linewidth Γ of the nuclear first-excited state are necessary. For ^{57}Fe, $\Gamma = 4.6 \times 10^{-9}$ eV. Such small quantities can be put in evidence by means of the Mössbauer effect, which we will recall very briefly. Basically the Mössbauer effect is the recoil-free emission and absorption of resonant gamma radiation. The experimental technique is most often based on the detection of the forward-scattered radiation emitted by a radioactive source after passing through a resonant absorber. The energy of the emitted photons can be modulated by moving the source with respect to the absorber. Suppose the absorber is a non-magnetic material in which the stable ^{57}Fe nuclei are incorporated in a cubic environment ('single-line absorber'). Each time the energy of the Doppler-modulated emitted photon coincides with the allowed transition in the absorber, a dip in the transmitted intensity will be observed. Thus the shape of the Mössbauer effect spectrum gives exact information on the radiated spectrum. To scan the natural linewidth of the first-excited state of ^{57}Fe, a velocity change of about 0.2 mm s^{-1} is needed. There are many articles and books describing the Mössbauer effect in detail [13].

Figure 5 gives the shape of Mössbauer spectra for a Zeeman-split source ($B_0 = 33$ tesla) consisting of an ensemble of rf-dressed nuclei ('dressing' in the ground state) and a single-line absorber. Results are shown for the case when $\beta = 0$ and the splitting parameter $\Delta = 4\Gamma$. Notice that, in general, the values of the splitting parameter Δ and the mixing angle α are both functions of the rf frequency ω and the magnitude of the rf magnetic

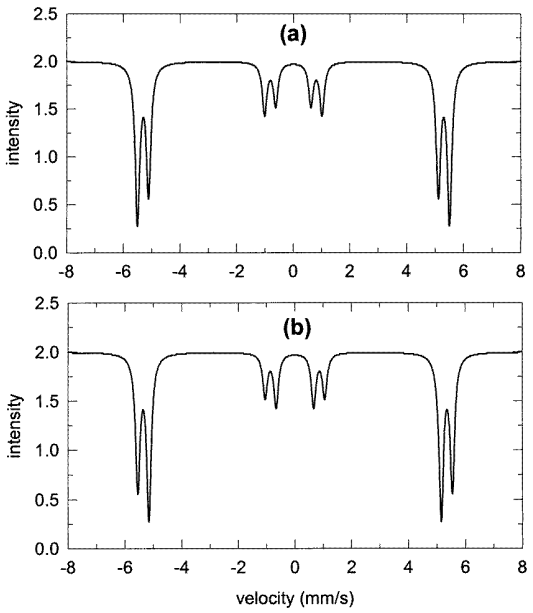

Figure 5. Mössbauer transition spectra using a Zeeman-split ^{57}Fe source and a single-line absorber when the photon direction is parallel to the Zeeman field in the presence of rf coupling in the ground state as in figure 4(a). In this case the rf radiation is off resonance; $\omega = 0.99\ \omega_g$ (a), and $\omega = 1.01\ \omega_g$ (b). Notice the asymmetry in the doublet dips.

flux density B_{rf}. Figure 5(a) shows the case when $\omega = 0.99\ \omega_g$ while figure 5(b) is for $\omega = 1.01\ \omega_g$. Notice the change in the asymmetry of the doublet peaks as the rf frequency is varied from below to above the resonant frequency. Figure 6 shows results similar to those of figure 5 except now $\beta = \pi/2$.

5. Discussion

Table 1 contains the complete information about the line intensities and energies of photons emitted by an ensemble of spin $3/2$ excited-state nuclei, embedded in a sample in which the Zeeman hyperfine magnetic field is constant in magnitude and direction, decaying to a nuclear spin $1/2$ ground state. The spin $1/2$ ground states are assumed to be coupled by a transverse rf radiation field. Table 1 gives the line intensities and photon energies for all emission directions and orientations of the Zeeman hyperfine magnetic field, assuming both lie in the plane perpendicular to the applied rf magnetic flux density. Table 1 also gives results for all coupling strengths of the two ground states expressed through the mixing angle α. The mixing angle α is determined by the ratio of the magnitude of the rf magnetic flux density to the Zeeman magnetic field, and the rf frequency. The Mössbauer spectra can be derived from the data of table 1 for all such configurations. For an arbitrary emission direction, in the above-mentioned plane, 12 different photons energies are possible. In general the Mössbauer spectrum consists of a series of doublet dips. The energy separation between dips of a doublet depends on the coupling strength between the two spin $1/2$ nuclear ground states and the rf field. This coupling strength is expressed as Δ. As Δ increases the separation between the doublet peaks increases. Furthermore the asymmetry of the dips in the doublets depends on the value of the rf frequency compared to the resonance frequency

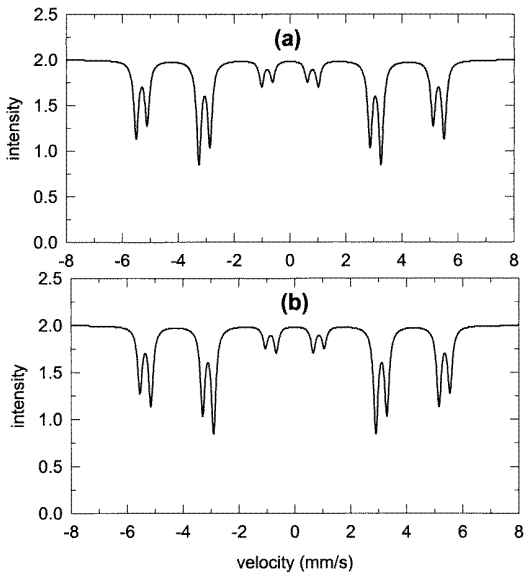

Figure 6. Mössbauer transition spectra using a Zeeman-split ^{57}Fe source and a single-line absorber when the photon direction is perpendicular to the Zeeman field in the presence of rf coupling in the ground state as in figure 4(b). In this case the rf radiation is off resonance; $\omega = 0.99\ \omega_g$ (a), and $\omega = 1.01\ \omega_g$ (b). Notice the asymmetry in the doublet dips.

ω_g. The characteristic shape of asymmetry in the dips will tell the experimenter whether the rf frequency is below or above the resonant frequency. It may prove possible to measure the ground state splitting or the rf frequency very accurately using this procedure.

It is interesting to note the agreement of some of our results with the corresponding cases obtained by Gabriel [14] (compare the upper half of figure 1 in [14] with our figure 3(b) and 6). The simulated spectra of figure 5 in [15] are also compatible with our results. The authors of [14] and [15] take a classical field approach to describe the rf field, as has already been mentioned.

In [16] the first Mössbauer experimental observation of Rabi splitting due to rf coupling of nuclear levels is demonstrated. They used a single line ^{57}CoRh source and an absorber in which the hyperfine sublevels of the Zeeman-split excited- or ground-state ^{57}Fe nuclei embedded in $Fe_{18}Ni_{82}$ are coupled by an rf field. Their theoretical results for the transverse rf-field application (see figure 1(d) in [16]) agree with ours. Their experimental results (see figure 2 in [16]) apply to the situation where there is a distribution of hyperfine magnetic fields, which broadens the spectrum. Our model can be adapted easily to take into account any distribution of hyperfine fields. Several other theoretical studies have been performed, all based on a classical radiation field [17–22]. For a brief summary see [6].

The main advantage of the model presented in this paper is that it gives simple analytical expressions for the line intensities and relative transition probabilities for the emitted photons in a transverse applied rf field when the sample has a constant Zeeman magnetic field perpendicular to the applied rf magnetic flux density and the emission direction is also perpendicular to the applied rf magnetic flux density. The Mössbauer spectra, for such cases, can be derived easily from these results. In the dressed-state model all operators are time independent. So the energy eigenvalues of the system are also time independent. Now the possible initial states of the system are nothing but the undressed states (given by (5) and (6)), not eigenstates of the total Hamiltonian. However these states can be expressed as

a linear combination of the eigenstates of the system. Since the eigenstates of the system are stationary states, the time evolution of the possible initial states of the system is easily obtained as indicated in section 3.3.

6. Conclusions

Based on the model of 'dressed nuclei' we have investigated the interaction of a transverse rf-radiation field with the ground-state Zeeman sublevels in the case of a ground-state nuclear spin $1/2$. This model considers the global quantum system of nuclei in a static hyperfine magnetic field and a quantized applied rf-radiation field in the Schrödinger picture. We have shown that when spontaneous emission occurs for this case via a magnetic dipole transition, for a nuclear excited-state spin $3/2$, it is possible that 12 different γ-transitions are produced. The energies corresponding to these transitions as well as the relative intensities are calculated for all directions of emission in the plane transverse to the rf magnetic flux density. The Mössbauer spectra, the source being an ensemble of dressed nuclei (ground-state 'dressing') and a single-line absorber, consist of, at most, 12 resonances for an arbitrary direction of emission. At exact resonance it is seen that each component of the original line (no rf) splits into a symmetric doublet. A treatment along the same lines could be used to study the spectrum when coupling occurs in the excited-state Zeeman sublevels. The expressions are expected to be more cumbersome, although the analysis should be straightforward. In fact, the most general case of rf coupling to the excited- or ground-state nuclear levels can be handled using the methods applied in this paper.

Acknowledgments

This work was supported by the IUAP-program IUAP P4-07, financed by the Belgian Federal Office for Scientific, Technical and Cultural Affairs and by FWO-Vlaanderen.

References

[1] Cohen-Tannoudji C and Haroche S 1969 *J. Physique* **30** 125
[2] Haroche S 1971 *Ann. Phys., Paris* **6** 189
[3] Cohen-Tannoudji C, Dupont-Roc J and Grynberg G 1992 *Atom–Photon Interactions* (New York: Wiley) p 407
[4] Odeurs J 1994 *Hyperfine Interact.* **92** 1043
[5] Odeurs J 1994b *Hyperfine Interact.* **92** 1051
[6] Odeurs J 1995 *Hyperfine Interact.* **96** 177
[7] Odeurs J 1997 *Hyperfine Interact.* **108** 535
[8] Baldwin G C and Solem J C 1997 *Rev. Mod. Phys.* **69** 1085
[9] Loudon R 1986 *The Quantum Theory of Light* (Oxford: Clarendon)
[10] de Shalit A and Feshbach H 1990 *Theoretical Nuclear Physics, Vol. I: Nuclear Structure* (New York: Wiley)
[11] Blatt J M and Weisskopf V F 1952 *Theoretical Nuclear Physics* (New York: Wiley)
[12] Hannon J P and Trammell G T 1969 *Phys. Rev.* **186** 306
[13] See, for example, Hoy G R 1992 *Encyclopedia of Physical Science* vol 10 (New York: Academic) pp 469–83
[14] Gabriel H 1969 *Phys. Rev.* **184** 359
[15] Salkola H and Stenholm S 1990 *Phys. Rev.* A **41** 3838
[16] Tittonen I, Lippmaa M, Ikonen E, Lindén J and Katila T 1992 *Phys. Rev. Lett.* **69** 2815
[17] Hack M N and Hamermesh M 1961 *Nuovo Cimento* **19** 546
[18] Mitin A V 1967 *Sov. Phys.–JETP* **25** 1062
[19] Krisnamurthy B and Sinha K P 1975 *J. Magn. Reson.* **17** 427
[20] Bashkirov Sh Sh and Sadykov E K 1978 *Sov. Phys.–Solid State* **20** 1988
[21] Oliaru S 1988 *Phys. Rev.* B **37** 7698
[22] Tittonen I, Javanainen J, Lippmaa M and Katila T 1993 *Hyperfine Interact.* **78** 397